6

Plasma treated bimetallic nanofibers as sensitive SERS platform and deep learning model for detection and classification of antibiotics

In the present chapter the functioning of an O_2 plasma treated bimetallic nanofibers as a new SERS platform is demonstrated. The performance of the designed SERS substrate has been initially evaluated with the standard Raman active probe molecules - BPE and R6G. For the standard Raman samples the LoD and LoQ of the proposed sensing platform have been estimated and the values are found to be 3.8 nM and 11.6 nM respectively. The EF of the designed sensing platform is calculated to be $\sim 10^8$ with a maximum signal variations of 5%. The applicability of the designed SERS substrate has been realized through detection of two antibiotics - FLU and LIN widely used in poultry farms. Furthermore, a deep learning model - ANN has been implemented for effective classification of the analyte molecules from a mixed sample.

6.1 Introduction

PVA nanofiber-based SERS substrates are widely used due to their easy fabrication procedure and excellent control over fabrication parameters. PVA is a water-soluble polymer recognized for its high thermal stability, tensile strength, and biodegradability [1, 2]. The primary problem associated with the conventional nanofiber preparation is the residual toxic chemicals; which occurs during the reduction of metals salts to form NPs. Again, NP aggregation is another issue which is commonly encountered in the chemical reduction methods. In this context, plasma treated nanofiber appears as a viable alternative to the conventional counterparts [3]. O_2 plasma-treated PVA nanofibers offer significant advantages over other nanofiber fabrication methods for SERS substrate fabrication, including superior nanoparticle binding, enhanced signal

uniformity, increased surface area, and improved hydrophilicity for analyte adsorption. These properties collectively contribute to higher sensitivity, greater reproducibility, and more reliable SERS measurements, especially when detecting trace-level analytes or operating in complex environments such as biological systems. The O_2 plasma treatment introduces oxygen-containing functional groups on the nanofiber surface, which facilitate the uniform and stable attachment of metal nanoparticles like gold or silver, creating more efficient SERS-active sites. This uniform nanoparticle distribution enhances signal consistency across the substrate, reducing variability and improving measurement accuracy. Moreover, the plasma treatment process significantly increases the surface roughness of the nanofibers, further enhancing surface area and generating more hotspots for Raman enhancement, resulting in superior detection sensitivity for low-concentration analytes. The improved hydrophilicity ensures better interaction and adsorption of water-based analytes, making the substrates particularly effective in applications where aqueous environments. Additionally, O_2 plasma treatment is a clean, solvent-free, and environmentally friendly technique, making it ideal for large-scale production without generating hazardous by-products.

In this work, a sensitive SERS platform has been demonstrated using plasma-treated bimetallic nanoparticle-decorated electrospun nanofibers. Unlike conventional nanofiber-based SERS substrates, the plasma-treated bimetallic nanofibers-based SERS platform offers high sensitivity and reproducibility characteristics. Additionally, the use of bimetallic nanoparticles contributes to both electromagnetic and chemical enhancement of SERS performance, while the plasma treatment facilitates controlled exposure of the embedded NPs to the analyte, thereby enhancing the overall sensitivity of the proposed technique. The designed SERS substrate has been employed to detect and analyse antibiotics in trace concentrations. The performance of the proposed SERS substrate was evaluated using standard Raman active samples BPE and R6G respectively. Upon observing its reliable performance with standard Raman active samples, its applicability has been demonstrated through the detection of two antibiotic drugs - FLU and LIN, widely used in poultry farms. The schematic of the proposed sensing work is depicted in figure 6.1.

For fabrication of the proposed SERS substrate, PVA solution has been mixed in a proportional amount with the bimetallic salt solution. Subsequently, the nanofibers obtained from the electrospinning unit were treated with O_2 plasma, where the metal salts were directly reduced to metal NPs. The presence of bimetallic NPs in the nanofiber supports electromagnetic enhancement for the scattered Raman signal from the analyte when it is brought into the vicinity of the hotspot regions of the NPs. Careful tuning of the voltage and rotational speed of the rotor during the electrospinning process enables deposition of nanofibers with a high surface area

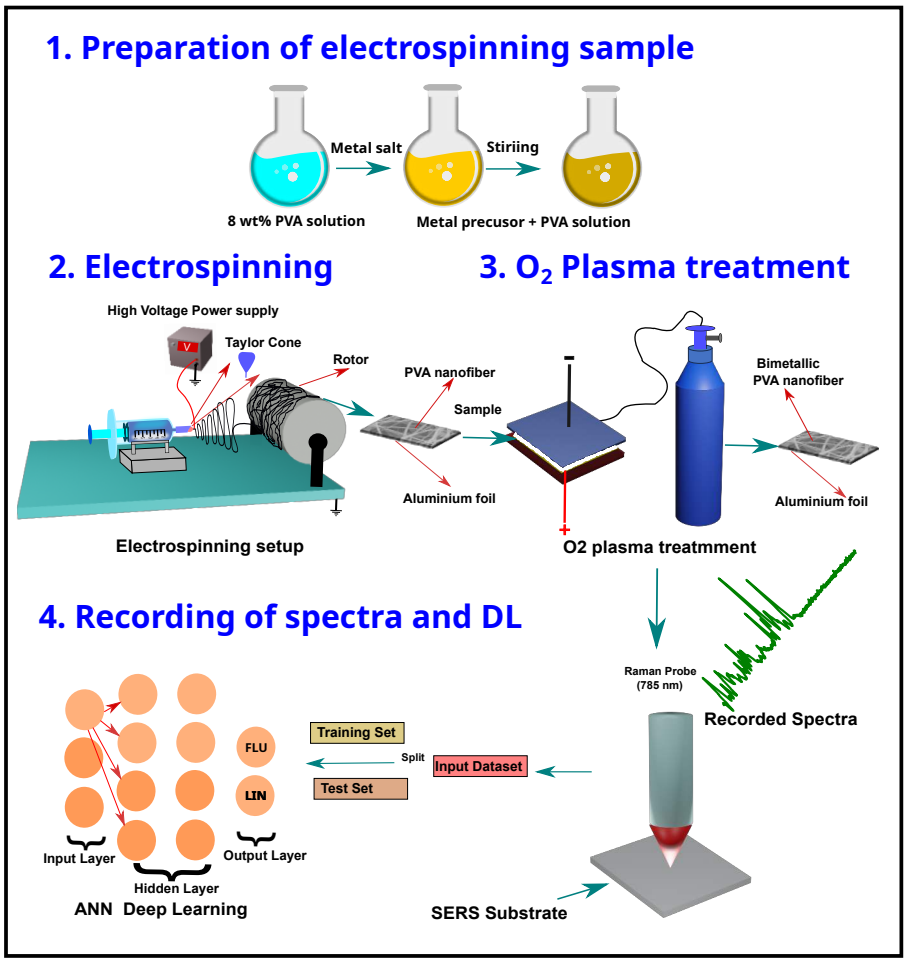

Figure 6.1: Schematic of the proposed sensing work

with controllable surface morphology. For the proposed SERS platform, the surface areas of the nanofibers facilitate interactions between analyte molecules and the localized plasmonic fields of the bimetallic NPs. Furthermore, due to the presence of oxygen-containing functional groups, the PVA nanofibers support chemical enhancement of scattered Raman signals, providing an additional enhancement to the sensing scheme. A deep learning-based model - ANN has been incorporated for classification of the targetted analytes FLU and LIN. ANN is a deep learning algorithm used for classification problems, employs a collection of connected units known as artificial neurons. The neural network is capable of segregating the data groups when complex datasets are involved [4]. SERS spectra can be highly non-linear, especially due to the complex molecular interactions and variations in the local environment of the analyte such as surface effects, orientation of molecules, or clustering. Some simple methods such as linear regression assumes a direct proportional relationship between the input and output variables which may not be adequate to capture the full complexity of the data. Neural networks, on the other hand, are highly suited to modelling non-linear relationships. The spectral signatures of the two antibiotics might overlap significantly, especially in real field samples. Linear regression might

struggle in distinguishing the differences of the overlapping peaks. A neural network can potentially learn to differentiate these signals more effectively by leveraging complex patterns in the data. The scheme was proposed in such a way that identification of the analyte molecules in trace concentrations involving complex mixtures could be performed.

Prior to implementing the ANN, PCA was performed to reduce the dimension into two specific datasets, also known as PCs, which were subsequently considered as inputs for the ANN model. The efficiency of the present model has been estimated using different machine learning metrics such as confusion matrix, variation of accuracy, and loss with the epoch cycles. Furthermore, the accuracy of the implemented ANN model has been compared with other ML techniques such as SVM, KSVM, and Naïve Bayes. A significant enhancement in the accuracy of results has been observed with the ANN model compared to the ML techniques. The use of ML and DL models in the proposed sensing scheme enables rapid and accurate identification of analytes, particularly in samples containing complex mixtures. The identification of individual analytes becomes challenging when overlapping peaks are present in the SERS spectra, as traditional methods may struggle to segregate the intricate spectral features. To address these challenges, ML and DL models, combined with dimensionality reduction techniques like PCA, offer reliable option. PCA and similar methods reduce the complexity of the data by identifying the most relevant features within the spectra, focusing on the variance that best represents the underlying chemical composition of the analytes. This feature extraction allows ML models to effectively process the data without relying on manual preprocessing or feature engineering, which can be labor-intensive, subjective, and prone to errors. By leveraging ML and DL, the system can automatically learn from the data, distinguishing between significant differences in spectral patterns. This not only speeds up the analysis but also increases the accuracy and robustness of the classification, even in the presence of overlapping spectral peaks. Furthermore, these models can handle the high dimensionality and complexity inherent to SERS data, allowing for the detection and classification of analytes in mixed forms.

6.2 Experimental

6.2.1 Chemicals

The chemicals $HAuCl_4 \cdot 3\,H_2O$, $AgNO_3$, PVA ($MM = 1{,}045{,}000\ gmol^{-1}$) were acquired from Merck, India. R6G and BPE were obtained from Alpha Aesar, India. All chemicals were utilized without any additional processing. The antibiotics, FLU and LIN were procured from a local medical store.

6.2.2 Preparation of the PVA solution and metal precursor solution

8 wt% PVA solution has been prepared in the laboratory by dissolving appropriate amount of PVA polymer in DI water. Precautions were taken to obtain a clear solution of PVA in DI water. To achieve this, 8 grams of PVA polymer was dissolved in 100 mL of DI water and stirring continuous for 5 hours. The final electrospinning solution was prepared by adding 1 mM of $AgNO_3$ and 0.01 mM of $HAuCl_4 \cdot 3\,H_2O$ to the PVA solution. Maintaining proper concentration ratios of the solvent is crucial to prevent reaction between the metal salts. During the fabrication process, it has been noted that high precursor concentration and low PVA concentration made it challenging to form nanofibers. At such conditions, the ejection of nanofibers from the syringe did not result in the formation of a Taylor cone [1]. Among various combinations of PVA bimetallic precursor ratios, the 3:1 volumetric ratio of PVA to metal precursor yielded the best results in terms of nanofiber deposition on the aluminium substrate and overall sensing performance.

6.2.3 Electrospinning and O_2 plasma setup

The electrospinning nanofiber unit (E-SPIN Nanotech Equipment, India) features an advanced solution delivery system equipped with precise pumps and a flow controller unit. This system ensures a controlled supply of polymer solutions, contributing to the consistency of nanofiber characteristics for the study. A dedicated high-voltage power supply (maximum $\sim$ 40 kV) is integrated that maintains a stable and adjustable electrostatic field, crucial for the formation of well-defined nanofibers. A microcontroller unit allows fine-tuning of spinning speeds (maximum $\sim$ 10,000 rpm) of the rotating drum, facilitating customization of the deposited nanofibers. A syringe (5 mL) loaded with a mixed polymer-metal salt solution maintained a flow rate of 0.5 mLh^{-1}. The ground collector is positioned at a distance of 15 cm from the needle tip. The optimum performance of the proposed SERS platform has been evaluated by varying the applied voltage and speed of the rotor drum; which are crucial for deposition of nanofibers over an aluminium foil. Figures 6.3(a) and 6.3(b) illustrate the variations in recorded Raman signals for different SERS substrates obtained by adjusting the applied voltage and rotational speed of the collector. The best SERS performance has been observed when maintaining the applied voltage and rotor speed at 22 kV and 1200 rpm, respectively, during the electrospinning process. The deposited nanofibers are then vacuum-dried for 1 hour before treating them in an O_2 plasma environment. The O_2 plasma treatment, conducted in a custom-built setup from Zeonics Systech, which utilizes a high-voltage dielectric barrier plasma generator supply with a tunable radio frequency controller unit, adjustable in the range of

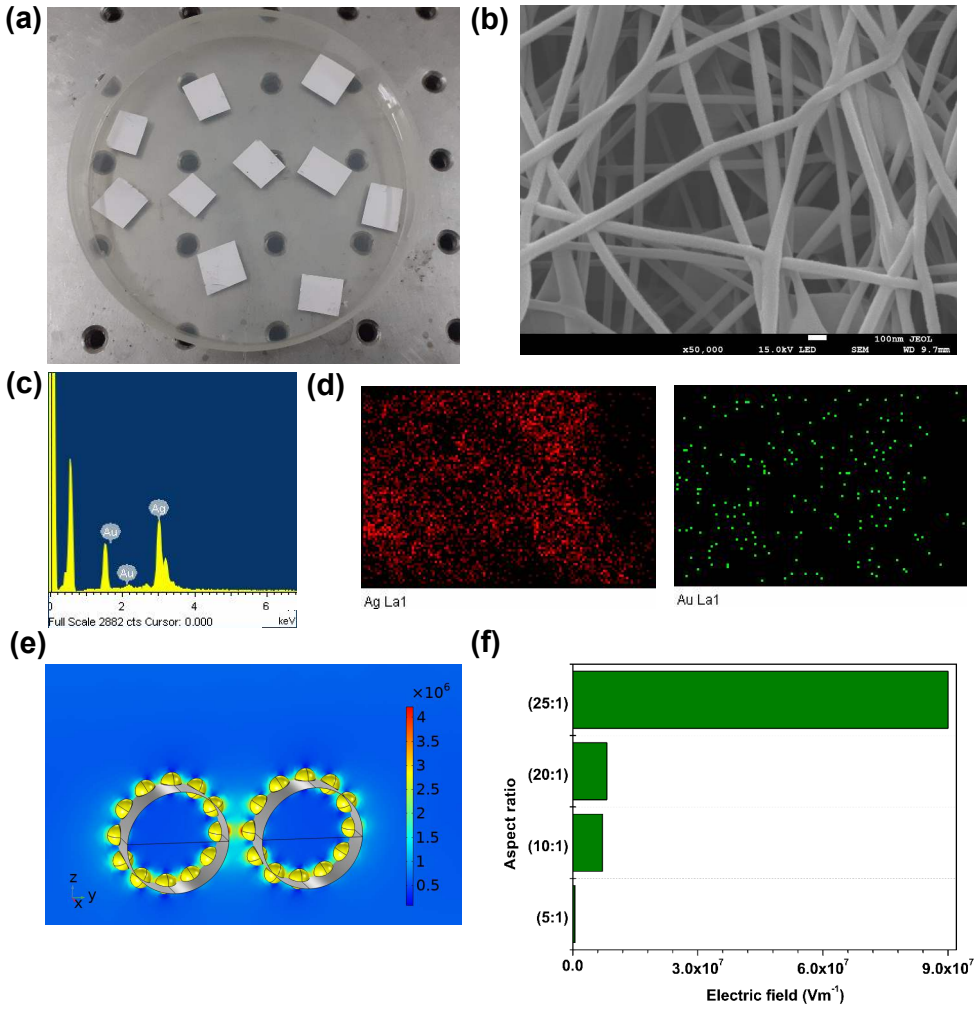

Figure 6.2: (a) Photo image of the fabricated SERS platform (b) FESEM image of the SERS substrate (scale bar is 100 nm) (c) EDX analysis of the SERS substrate confirming the presence of Au, Ag (d) elemental mapping of AgNPs and AuNPs over the fabricated SERS platform showing the distribution of particles (e) COMSOL Multiphysics simulation of the SERS substrate showing the amplitudes of the coupled EM field generated in the hotspot region of the SERS substrate; the incident electric field amplitude was assumed as 6.4×10^4 Vm^{-1} (f) Variation of the coupled EM field with the aspect ratio of nanofibers.

0 to 50 kV at 25 mA. The O_2 plasma in the reactive chamber etches the nanofiber surface, exposing embedded nanoparticles. Figure 6.2(a) displays a photo image of the fabricated SERS substrate, while figure 6.2(b) presents the FESEM image of the deposited nanofibers. Figure 6.2(c) shows the EDX of the proposed SERS platform, indicating the presence of AuNPs and AgNPs in the fabricated nanofibers. Figure 6.2(d) depicts the elemental mapping of the designed SERS substrate, demonstrating the uniform distribution of nanoparticles over the sensing region of the proposed SERS platform.

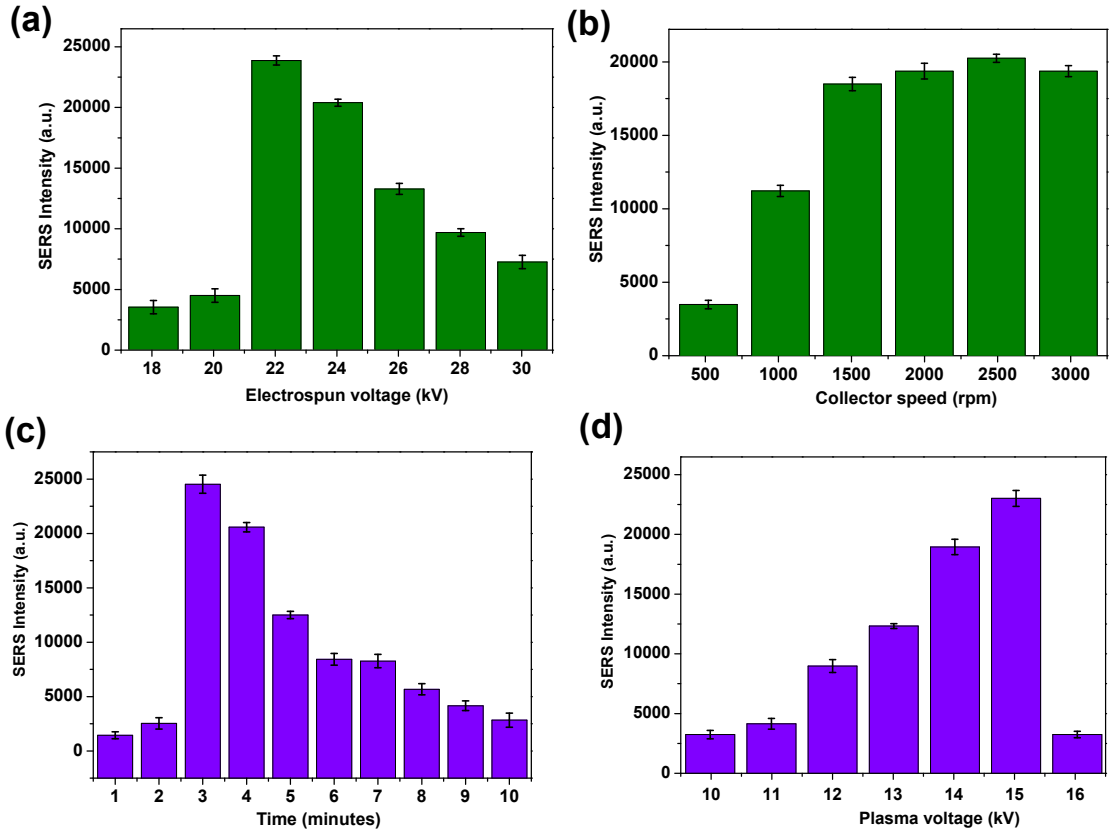

Figure 6.3: (a) Variation of the SERS signal intensity with the electrospinning voltage for the signature Raman peak of BPE near 1199 cm^{-1} (b) Variation of the SERS signal intensity with the rotational speed of the ground collector for the signature Raman peak of BPE near 1199 cm^{-1} (c) Variation of the SERS signal intensity with the plasma etching time for the signature Raman peak of BPE near 1199 cm^{-1} (d). Variation of the SERS signal intensity with plasma voltage corresponding to the signature Raman peak BPE near 1199 cm^{-1} ; (Error bars are plotted using the standard deviation, calculated from five repetitions for each sample)

6.2.4 Raman spectrometer and data analysis

The specification of the Raman instrumentation has been incorporated in the section 2.2.4. All the machine learning and deep learning algorithms were implemented using the Keras package in R programming language [5].

6.2.5 EM simulation

EM simulations has been performed to estimate the coupled EM field amplitude for the designed SERS substrate using the COMSOL Multiphysics software (wave optics module). The simulation software employs the finite element method based on Maxwell's electromagnetic equations to estimate the amplitude of the coupled EM intensity at the nanoparticle site upon excitation by the incident laser beam. Figure 6.2(e) illustrates the distribution of the coupled EM field amplitude near the hotspots of the nanofibers. The simulation was performed by depicting the FESEM image of

the designed SERS substrate. For this, the nanofibers of diameter 20 nm and length 124 nm have been considered to estimate the amplitude of EM field. The amplitude of the coupled EM field was estimated to be 7.1×10^6 Vm^{-1} while the amplitude of the incident EM field was assumed as $6.4 \times 10^4\,Vm^{-1}$. Additionally, EM simulations were conducted to investigate the effect of nanofiber aspect ratio on the coupled EM field for the designed SERS substrate. The aspect ratio significantly influences Raman band enhancement, with higher aspect ratio fibers exhibiting increased hotspot regions between adjacent nanofibers, resulting in greater enhancement to the SERS signal compared to lower aspect ratio counterparts. Figure 6.2(f) illustrates the variation in coupled EM field amplitude with varying aspect ratios of the nanofibers. The results indicate that nanofibers with the highest aspect ratio would yield the maximum amplitude for the coupled electromagnetic field (9×10^7 Vm^{-1}). The details of EF, estimated through both simulation and experimental methods, are described in table 8.16.

6.3 Results and Discussion

6.3.1 Optimization of the SERS substrate

At the outset of the current sensing study, the performance of the proposed SERS platform has been optimized by adjusting parameters related to the O_2 plasma treatment unit. Different durations of O_2 plasma etching has been conducted, and the performance were evaluated by recording SERS spectra from a test Raman probe, BPE, at a concentration of 1 µM. Figure 6.3(c) illustrates the variations in scattered Raman signal intensities for the signature Raman band at 1199 cm^{-1} of BPE, recorded from ten different SERS substrates that were treated at different durations in O_2 plasma environment. Among the different durations of O_2 plasma treatment, optimal SERS performance has been noticed for 3-minute treatment. The size of the generated bimetallic NPs depends on the plasma etching time, subsequently influencing the performance of the designed SERS platform [5]. Short plasma exposure may not sufficiently reduce metal precursors to form NPs, while prolonged exposure may damage the nanofiber surface morphology, thus affecting performance. Furthermore, SERS performance was assessed at varying plasma discharge voltages, shown in figure 6.3(d). The proposed SERS substrate exhibited optimal performance at a plasma voltage of 15 kV. For subsequent experimental work, plasma etching time and plasma discharge voltage were maintained at 3 minutes and 15 kV, respectively.

6.3.2 SERS analysis of BPE and MG

Following the optimization phase, analysis of Raman signals from standard Raman-active probe molecules, BPE and R6G have been performed. Stock solutions of BPE and R6G were prepared in the laboratory by dissolving a specified amount in DI water. The lower concentration samples were obtained by diluting the stock solutions with an appropriate proportion of DI water. Figure 6.4(a) presents the SERS spectra of BPE at a concentration of 1 µM before and after plasma treatment.

The figure clearly demonstrates the enhancement in scattered Raman signal intensities upon exposing the substrate to O_2 plasma. O_2 plasma induces the formation of AuNPs and AgNPs, thereby generating hotspot regions on the SERS substrate. Figure 6.4(a) illustrates the characteristic Raman bands of BPE when recorded from the proposed SERS substrate with and without treatment under O_2 plasma. For reference, the figure includes the Raman signature of BPE recorded from a blank nanofiber substrate. It is evident from the figure that the proposed SERS platform yields the highest SERS signal intensities upon exposure to O_2 plasma. Figures 6.4(b) and 6.4(c) depict the relative signal intensities for BPE and R6G, respectively, recorded at different concentrations of the samples. These figures clearly show that the intensities of the Raman bands from the target analytes increase with the increment in concentrations. The Raman band assignments for BPE and R6G are provided in the appendix section (see tables 8.3 and 8.1). Linear regression analysis has been performed for both BPE and R6G. Figure 6.4(d) and figure 6.4(e) illustrate the variation of normalized SERS signal intensity at varying concentrations of the analytes in the range of 10 nM to 100 nM. The R^2 values for BPE and R6G were estimated to be 0.996 and 0.991, respectively. These high R^2 values suggest a good linear correlation between the variations in Raman signal intensity and the concentration of analytes.

6.3.3 Estimation of LoD and LoQ

With BPE as test Raman probe, the LoD for the designed sensing platform has been estimated using equation 2.1 and the value was found to be 3.8 nM. Again, the limit of quantification (LOQ) for the present sensing scheme is estimated using equation 6.1.

$$LoQ = \frac{10\sigma}{S} \tag{6.1}$$

where, σ is the standard deviation of the response and S is the slope of the calibration curve. The LoQ of the fabricated SERS substrate is estimated to be 11.6 nM

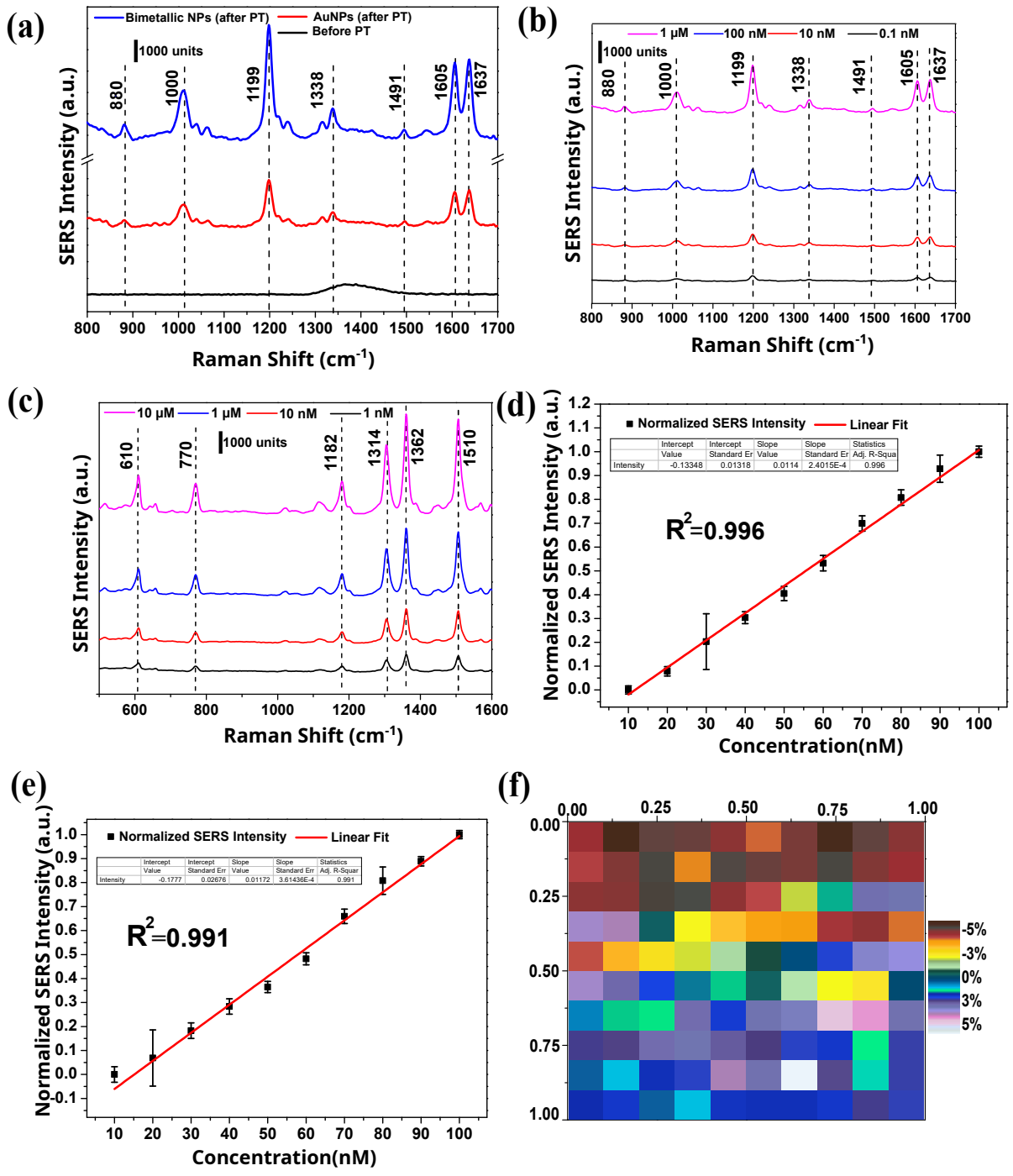

Figure 6.4: (a) Comparison of scattered Raman signal between before and after O_2 plasma treatment (PT) (b) Variation of the intensities of the Raman bands with change in concentration of the BPE (c) Variation of the intensities of the Raman bands with change in concentration of the R6G (d) Linear regression analysis of the normalized SERS signal intensity with the concentration of the BPE (e) Linear regression analysis of the normalized SERS signal intensity with the concentration of the R6G (f) Raman mapping of the fabricated SERS platform corresponding to the signature Raman peak near 1199 cm^{-1}; (Error bars are plotted using the standard deviation, calculated from five repetitions for each sample)

6.3.4 Estimation of EF

The EF of the proposed sensing scheme has also been estimated using equation 2.2, and the value is found to be $\sim 10^8$. Table 6.1 depicts the SERS performance of the proposed sensing scheme alongside some of the previously reported works on plasma-treated nanofiber-based SERS substrates.

Table 6.1: Performance comparison of the present SERS platform with other reported works on plasma treated nanofiber-based SERS substrates

Substrate	Analyte	EF	RSD (%)	LOD (nM)	Reference
AgNP/poly(methyl methacrylate) (PMMA)	4-Mercaptobenzoic acid (4-MBA)	$\sim 10^5 - 10^6$	Not specified	Not specified	[6]
AgNP/poly(L-lactide) (PLLA) & AgNP/PAN	4-aminothiophenol crystal violet R6G	Not specified	19.9%	1	[7]
This work	BPE, R6G, FLU LIN	10^8	5%	3.8	Present work

6.3.5 Study of uniformity and reproducibility characteristics

The uniformity characteristics of the proposed SERS substrate has been evaluated through mapping the characteristic Raman peak of BPE near 1199 cm^{-1} over the sensing region of the SERS substrate. For this, 1 µM of BPE has been dispensed over the sensing area of the SERS substrate, and the scattered Raman signals were recorded in a spectral array of 10×10. Figure 6.4(f) depicts the spectral mapping of BPE for its characteristic Raman band at 1119 cm^{-1}. A reasonably stable Raman signal has been observed with signal fluctuations of $\sim 5\%$, suggesting a good uniformity characteristics of the proposed sensing platform. Additionally, a reproducibility study has been conducted by utilizing R6G as a test analyte for five identical substrates. For each substrate, SERS spectra have been recorded from five random points, and the mean values have been considered. Figure 6.5 illustrates the reproducibility study of the designed SERS platform and a maximum RSD of $\sim 6\%$ has been observed. This again indicates that the proposed sensing scheme is highly reproducible in nature.

6.3.6 SERS analysis of antibiotics

The applicability of the proposed sensing platform has been demonstrated through trace detection and analysis of two antibiotic samples FLU and LIN. First, a stock solution of 10 ppm was prepared in DI water and another three more samples were prepared by diluting the stock solution. 10 µL each of the prepared analyte samples

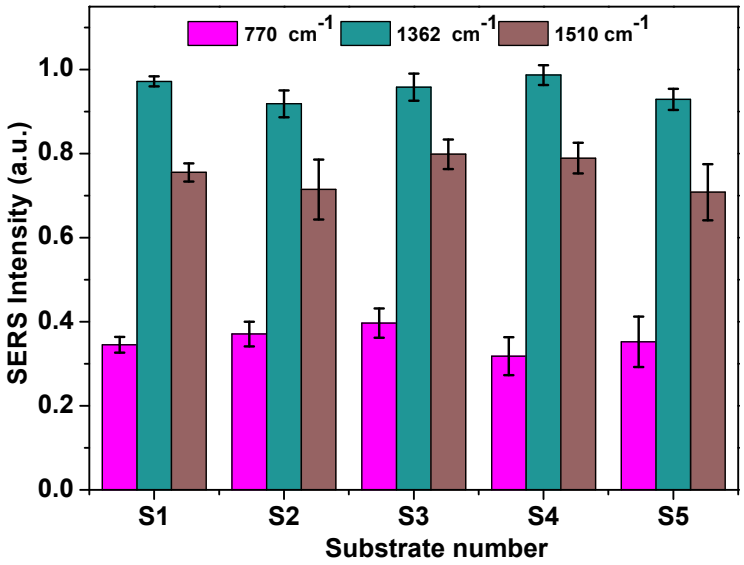

Figure 6.5: Reproducibility study of the fabricated SERS platform; (Error bars are plotted using the standard deviation, calculated from five repetitions for each sample)

have been dispensed over the sensing region and the SERS spectra were recorded

Figure 6.6(a) and 6.6(b) depict the SERS spectra of FLU and LIN recorded by the Raman spectrometer. The figures clearly illustrate that the signal intensities of the characteristic Raman bands of the targeted analytes increase with the increment in concentrations of the samples. The band assignments for the considered analytes have been included in the appendix (Table 8.14, Table 8.15). Linear regression analysis of the targeted antibiotics was also conducted, yielding values of 0.973 and 0.998 for FLU and LIN, respectively. The high values of R^2 again signify a strong linear correlation between the normalized SERS signal intensity and the concentration of the analyte sample. The concentration of unknown samples for FLU and LIN can be estimated using the following regression equations.

$$Concentration\ of\ FLU = \frac{Normalized\ SERS\ signal\ Intensity - 0.038}{1.092} \tag{6.2}$$

$$Concentration\ of\ LIN = \frac{Normalized\ SERS\ signal\ Intensity - 0.422}{1.447} \tag{6.3}$$

For the proposed sensing platform, LoDs for FLU and LIN were estimated to be 0.1 ppm and 0.3 ppm, respectively. According to the Food and Agricultural Organization of the United Nations (FAO), the MRL for FLU and LIN are set to be 100 ppm and 50 ppm, respectively. Thus, with the proposed sensing scheme, it is possible to detect these analytes well below the permissible MRL specified by the FAO [8].

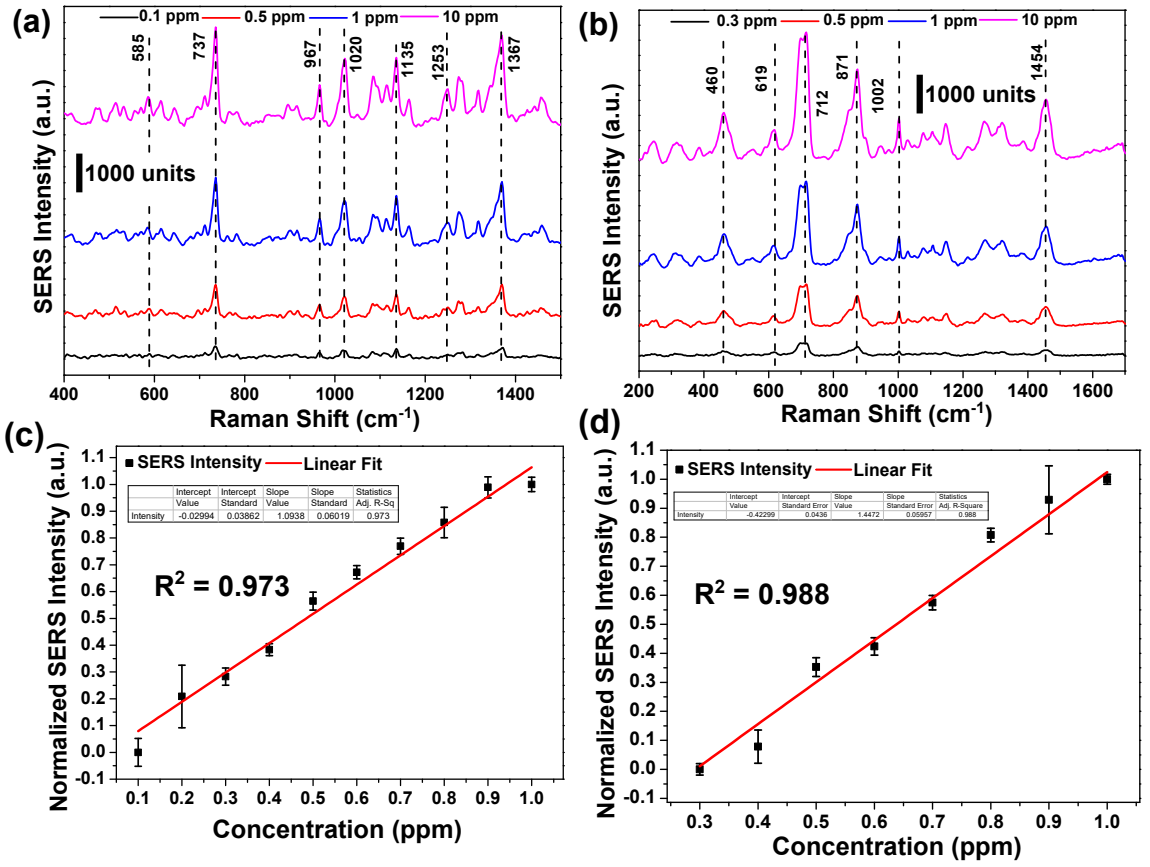

Figure 6.6: (a) Variation in the intensities of the Raman bands with the concentration of FLU (b) Variation in the intensities of the Raman bands with the concentration of LIN (c) Variation of the intensities of the Raman bands with change in concentration of the FLU (d) Variation of the intensities of the Raman bands with change in concentration of the LIN; (Error bars are plotted using the standard deviation, calculated from five repetitions for each sample)

6.3.7 Implementation Machine learning

In the final step of the present sensing work, the ANN model has been implemented to classify FLU and LIN samples from the mixed matrices. ANN is a deep learning algorithm for classification problems. Prior to performing the ANN, the spectral data were fed into the PCA algorithm to reduce the dimension of the dataset. The most prominent principal components (PC 1, PC 2) were considered, and these obtained PCs were then used as the input for the ANN model. For training set, 70% of the total dataset was used, while the remaining 30% has been used as the test set. From the training set data, 20% of the data were used for validation of the ANN model. The model was built with 8 hidden layers, and a batch size of 10 was considered in each epoch. Figure 6.7(a) shows the PCA-ANN plot for the proposed sensing data, indicating a clear segregation of the analyte samples in the PCA plot, validating the effectiveness of the developed model. Figure 6.7(b) shows the loss and accuracy of the model with the epoch numbers, indicating a decreasing trend in the loss and increasing trend in the accuracy, with the accuracy stabilized after 250 epochs. Figure

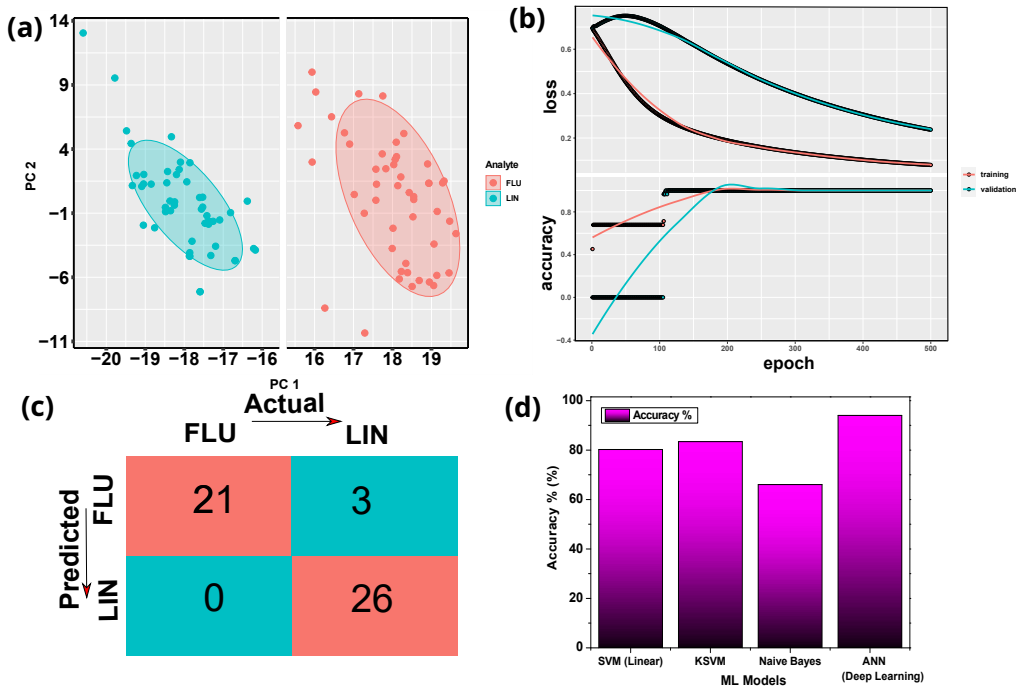

Figure 6.7: (a) PCA-ANN based classification of the Analytes FLU and LIN (b) Comparison of loss and accuracy with the number of epochs for training and validation data (c) Confusion matrix of the developed PCA-ANN scheme (d) Comparison of the accuracy of different ML modalities with deep learning ANN scheme

6.7(c) shows the confusion matrix of the ANN classification, depicting the correct predictions in the diagonal, while the off-diagonal elements represent the incorrect predictions. From the confusion matrix, it is evident that the PCA-ANN model yields a good degree of classification accuracy with the optimized parameters in the algorithm. The performance of the present ANN model has been compared with other ML-based models, and the results are depicted in figure 6.7(d), clearly indicating that compared to the other ML-based models, the present ANN algorithm yields higher classification accuracy.

The incorporation of deep learning model supports rapid identification of the analyte molecules from mixed matrices. Deep learning models (ANNs) are especially suitable for handling complex, non-linear relationships in spectral data. They can automatically learn hierarchical representations of features, capturing intricate patterns which might be challenging for ML-based models like SVM or Naive Bayes [9]. ANNs can automatically learn relevant features from the raw data, reducing the need for extensive manual feature engineering. In contrast, SVM and Naive Bayes may require more feature engineering to achieve good performance.

6.4 Summary

In summary, a novel SERS platform achieved via O_2 plasma treatment of bimetallic PVA electrospun nanofibers has been presented. The present work demonstrates its effectiveness in detecting and analyzing antibiotics, specifically FLU and LIN. The method proposed employs a green synthesis approach, where metal precursors were reduced through plasma etching process. To facilitate rapid classification and identification of analytes within mixed samples, an optimized deep learning algorithm, namely an ANN model has been implemented. The developed sensing approach offers a cost-effective, swift, and reliable method for analyzing samples within complex mediums. Despite the fact that the proposed sensing platform is effective in sensing of target analyte in trace concentrations, the fabrication of nanofibers is a relatively complex process. It depends on several parameters like polymer concentration, viscosity, evaporation rate, interfacial interaction, applied voltage, and flow rate. Even though the surface morphology of the electrospun PVA nanofibers can be tuned by changing the applied bias voltage and the collector configuration, it may vary in different environments. For instance, ambient conditions like humidity and local temperature may cause a change in the optimization parameters for the deposition of the nanofiber and hence may yield a variation in the surface morphology for the deposited nanofibers. This may subsequently lead to variations in SERS performance. The fluctuations in intensities of the Raman bands in different regions of the SERS substrate pose difficulty for reliable and quantitative estimation of the analyte samples. The plasma exposure time plays a critical role in determining the size of the generated NPs. Also, for longer duration of plasma treatment, the nanofibers may get damaged. An optimized etching time is highly desirable to obtain a sensitive SERS platform. To implement the present sensing scheme for field-collected applications, proper binding agents or functionalization of the analytes with the NPs may be required to improve the selectivity for a specific targeted sample. This opens another scope for further studies for the present sensing work.

References

[1] Pan, X., Bai, L., Pan, C., Liu, Z., and Ramakrishna, S. Design, Fabrication and Applications of Electrospun Nanofiber-Based Surface-Enhanced Raman Spectroscopy Substrate. *Critical Reviews in Analytical Chemistry*, pages 1–20, 2021. Publisher: Taylor & Francis.

[2] Agarwal, S., Wendorff, J. H., and Greiner, A. Chemistry on electrospun polymeric nanofibers: merely routine chemistry or a real challenge? *Macromolecular rapid communications*, 31(15):1317–1331, 2010.

[3] Yadav, S. and Satija, J. The current state of the art of plasmonic nanofibrous mats as SERS substrates: design, fabrication and sensor applications. *Journal of Materials Chemistry B*, 9(2):267–282, 2021.

[4] Erzina, M., Trelin, A., Guselnikova, O., Dvorankova, B., Strnadova, K., Perminova, A., Ulbrich, P., Mares, D., Jerabek, V., Elashnikov, R., et al. Precise cancer detection via the combination of functionalized SERS surfaces and convolutional neural network with independent inputs. *Sensors and Actuators B: Chemical*, 308:127660, 2020.

[5] R Core Team, R. R: A language and environment for statistical computing. 2013.

[6] Bao, Y., Lai, C., Zhu, Z., Fong, H., and Jiang, C. SERS-active silver nanoparticles on electrospun nanofibers facilitated via oxygen plasma etching. *RSC advances*, 3(23):8998–9004, 2013.

[7] Liu, Z., Jia, L., Yan, Z., and Bai, L. Plasma-treated electrospun nanofibers as a template for the electrostatic assembly of silver nanoparticles. *New Journal of Chemistry*, 42(13):11185–11191, June 2018. ISSN 1369-9261. doi: 10.1039/C8NJ01151F. URL https://pubs.rsc.org/en/content/articlelanding/2018/nj/c8nj01151f. Publisher: The Royal Society of Chemistry.

[8] Alimentarius, C. Maximum residue limits (MRLs) and risk management recommendations (RMRs) for residues of veterinary drugs in foods. *Cac/Mrl*, pages 2–2015, 2018.

[9] Korotcov, A., Tkachenko, V., Russo, D. P., and Ekins, S. Comparison of Deep Learning With Multiple Machine Learning Methods and Metrics Using Diverse Drug Discovery Data Sets. *Molecular Pharmaceutics*, 14(12):4462–4475, Dec. 2017. ISSN 1543-8384, 1543-8392. doi: 10.1021/acs.molpharmaceut.7b00578. URL https://pubs.acs.org/doi/10.1021/acs.molpharmaceut.7b00578.